

Safety and feasibility of fat injection therapy with adipose-derived stem cells in a rabbit hypoglossal nerve paralysis model: A pilot study

Akihisa Wada, MD¹, Naoki Nishio, MD, PhD^{1,2}, Sayaka Yokoi, MD¹, Hidenori Tsuzuki, MD¹, Nobuaki Mukoyama, MD, PhD¹, Takashi Maruo, MD, PhD¹, Mariko Hiramatsu, MD, PhD¹, Tokunori Yamamoto, MD, PhD³, Momokazu Goto, MD, PhD³, Yasushi Fujimoto, MD, PhD¹, Michihiko Sone, MD, PhD¹

1 Department of Otorhinolaryngology, Nagoya University Graduate School of Medicine, Nagoya, Japan;

2 Department of Otolaryngology-Head and Neck Surgery, Stanford University School of Medicine, Stanford, CA, United States;

3 Department of Urology, Nagoya University Graduate School of Medicine, Nagoya, Japan.

Running title: Fat injection therapy with adipose-derived stem cells

Address for correspondence: Naoki Nishio, MD, PhD

Department of Otorhinolaryngology, Nagoya University Graduate School of Medicine, 65, Tsurumai-cho, Showa-ku, Nagoya 466-8550, Japan.

Phone: +11-81-52-744-2323, fax: +11-81-52-744-2325

E-mail: naokin@med.nagoya-u.ac.jp

Safety and feasibility of fat injection therapy with adipose-derived stem cells in a rabbit hypoglossal nerve paralysis model: A pilot study

Abstract

Objective: The aim of this study is to establish a unilateral tongue atrophy model by cutting the hypoglossal nerve and to evaluate the safety and feasibility of a fat injection of adipose-derived stem cells (ADSCs) to restore swallowing function.

Methods: A total of 12 rabbits were randomized to three groups; the ADSCs+fat group (n=4), the fat group (n=4) and the control group (n=4). All rabbits were treated with denervation of the left hypoglossal nerve and their conditions including body weight and food intake were checked during follow-up periods (8 weeks). At 4 weeks after the transection of the nerve, rabbits received the injection therapy into the denervated side of the tongue with 1.0mL fat tissue premixed with 0.5mL ADSCs in the ADSCs+fat group, 1.0mL fat tissue premixed with 0.5mL PBS in the fat group and 1.5mL PBS in the control group. Rabbits were euthanized 8 weeks post-treatment and resected tongues were collected, formalin-fixed and paraffin embedded. To evaluate the change of the intrinsic muscles of the tongue, muscle fibers around the treatment area was analyzed by evaluating 5 consecutive hematoxylin-eosin slides per rabbit.

Results: Food intake did not decrease upon nerve denervation, and none of the rabbits displayed adverse effect such as aspiration, surgical wound dehiscence or infection. No significant body weight changes were found between the three groups at 4 and 8 weeks after nerve transection ($p>0.05$). In the control group, the denervated side of tongue had

significantly smaller muscle fiber areas and diameters compared to the non-denervated side ($p < 0.05$). The ADSCs+fat group demonstrated a larger area of inferior longitudinal muscle fibers compared to the control and the fat groups ($582 \pm 312 \mu\text{m}^2$ vs. $405 \pm 220 \mu\text{m}^2$ and $413 \pm 226 \mu\text{m}^2$; $p < 0.05$). A significant thicker lesser diameter of inferior longitudinal muscle fibers was found in the ADSCs+fat group compared to the control and the fat groups ($24 \pm 8 \mu\text{m}$ vs. $20 \pm 6 \mu\text{m}$ and $20 \pm 7 \mu\text{m}$; $p < 0.05$).

Conclusion: The rabbit tongue atrophy model was found suitable for the assessment of muscle change after nerve transection. Fat injection therapy with ADSCs demonstrated great potential to prevent the muscle atrophy after denervation and to promote the muscle regeneration around the injection area.

Keywords: fat injection, adipose-derived stem cell, swallowing disorder, hypoglossal nerve paralysis, rabbit

INTRODUCTION

The swallowing system comprises both the neurological and functional system and is affected by a great variety of diseases including, but not limited to, neuromuscular diseases and head and neck cancer. Swallowing pressure plays a critical role to ensure safe transportation of a food and water without aspiration and when having a swallowing disorder, there is a dysfunction of the combined movement of the oral cavity, pharynx and esophagus which has been associated with aspiration, severe nutritional and respiratory complications, and in some cases results in death [1]. Although the actual prevalence of dysphagia remains unknown, 15% of the elderly population is thought to be affected by dysphagia [2].

Particularly, insufficient swallowing pressure during the oral and pharynx phase often leads to severe aspiration pneumonia, which remarkably worsens the quality of life due to the lack of eating [3]. To restore swallowing pressure when eating food, various surgical interventions have been proposed such as laryngeal suspension, cricopharyngeal myotomy and vocal fold medialization [4,5]. However, despite the usefulness of these surgical procedures to change the anatomical structure from the inner or outer side, adequate swallowing pressure during the oral and pharynx phase remains challenging in patients with absolute volume loss of the head and neck organs.

Fat injection therapy is a technique for transplanting autologous fat cells and is extremely suitable for filling tissue defects due to its safety (no risk of potential graft vs. hosts reaction) and easy access to fat cells for harvesting [6]. In the head and neck region, autologous fat injection therapy is commonly used for unilateral vocal fold paralysis and is ideal when the glottic gap is relatively small [7]. The technique consists of

transplantation of not only living fat cells but also adipose-derived stem cells (ADSCs) and many growth factors, which means that the fat injection has a potential of regenerative properties in the harvested adipose tissue. Previously, we demonstrated that high concentration of ADSCs added to autologous fat injection therapy led to increased blood flow and remarkable hypertrophy of the muscle fiber in the area surrounding injection site in unilateral vocal fold paralysis in large animal [8]. Although fat injection therapy is recognized as a feasible treatment for unilateral vocal fold paralysis in the clinical setting [9], little attention has been paid to using this technique to improve swallowing disorder in the oral and pharynx regions [10,11].

We hypothesize that the fat injection therapy, including a high concentration of ADSCs, has great potential to improve the swallowing disorder in patients with a loss of the volume in head and neck region. To demonstrate the feasibility of this approach, in a preclinical study a unilateral tongue atrophy model was developed by cutting the hypoglossal nerve. Subsequently the safety and feasibility of fat injection with ADSCs in this rabbit-based hypoglossal nerve paralysis model was assessed for restoring swallowing disorder.

MATERIALS AND METHODS

Study Overview

The animal care and the study protocol were approved by Institutional Animal Care and Use Committee (29455). The workflow of this study is demonstrated in Fig. 1a. A total of 12 male Japanese white rabbits (weighing 2.4-2.6kg) were treated with denervation of the left hypoglossal nerve. Animals were randomized to three groups; the

ADSCs+fat group (n=4), the fat group (n=4) and the control group (n=4).

At 4 weeks after the transection of the nerve, the injection therapy was orally performed in the denervated side of the tongue. Rabbits received an injection of 1.0mL fat tissue premixed with 0.5mL ADSCs in the ADSCs+fat group, 1.0mL fat tissue premixed with 0.5mL PBS in the fat group and 1.5mL PBS in control group. At 8 weeks post-treatment, all rabbits were euthanized using an overdose of sodium pentobarbital.

Food intake and general condition were carefully checked every day from the moment of denervation up to the day of euthanasia. Similarly, the body weight was measured once per week and recorded.

Unilateral hypoglossal nerve paralysis model

Under general anesthesia rabbits were secured in a spine position and a horizontal skin incision was made around the neck area. The hypoglossal nerve was surgically exposed and the nerve transection was performed with removal of a 1 cm nerve segment completely after the confirmation of the fasciculation in the denervated side of the tongue (Fig. 1b) to produce the hypoglossal nerve paralysis model. After the nerve transection, the proximal and distal edges of left hypoglossal nerve were ligated by nonabsorbable surgical suture to prevent the elongation and regeneration of hypoglossal nerve.

Fat injection therapy for tongue

At 4 weeks after the transection of the nerve, rabbits were brought back to the operation room, and anesthetized as described above. After confirmation of atrophy and fasciculation of the denervated side of the tongue, a skin incision around the left groin

was performed and subcutaneous fat tissue was harvested by direct excision. Harvested adipose tissue was washed and minced finely into particles. A total amount of 1.5mL was mixed and loaded in a retrograde fashion into a 3.0mL disposable syringe (Fig. 1c).

After the tissue preparation, the rabbit tongue was retracted from the oral cavity until the circumvallate papillae were visible. The injection therapy was then orally performed at 2cm posterior from tongue tip on the denervated side of the tongue using a syringe with a 18-gauge needle with direct observation (Fig. 1d). To avoid leakage of the fat from the injection site, a cotton swab was pressed over the injection site for 5 min after fat injection.

Isolation and Culture of ADSCs

To isolate and culture rabbit ADSCs, adipose tissue was harvested from the inguinal area at the same time of the nerve transection in the ADSCs+fat group (n=4). Harvested adipose tissue was washed with PBS and minced finely into particles. Culture of ADSCs was performed as previously reported by Gautam [12]. Briefly, the adipose tissue was digested with 0.3% Collagenase Type I (GIBCO, Grand Island, USA) for 90 min at 37°C with moderate shaking. After shaking, the cell suspension was centrifuged at 1300 rpm for 5 min, and then, the supernatant was discarded. The pellet was suspended with 20mL of the culture medium composed of Mesen PRO RS (GIBCO, Grand Island, USA) supplemented with 10% Fetal Bovine Serum (GIBCO, Grand Island, USA) and 1% penicillin–streptomycin (Pen Strep, GIBCO, Grand Island, USA). The cells were incubated at 37°C in humid air with 5% CO₂ for 7 days. After seeding, we simply harvested the attached and proliferated cells. The cells were detached with 0.25% trypsin–

ethylenediaminetetraacetic acid solution and washed by centrifugation at 1300 rpm for 5 min through a culture medium. Finally, a total of 2.0×10^6 ADSCs in 0.5mL PBS were prepared and injected in the ADSCs+fat group.

Histological assessment

Rabbit tongues were dissected out and fixed in 4% paraformaldehyde (Fig. 2a). Tongues were then breadloafed in 5mm thick tissue sections in the coronal plane from the tongue tip to tongue base for precise evaluation of intrinsic muscle fibers in the tongue (Fig. 2b). All tissue sections were cassetted and embedded in paraffin after which $4\mu\text{m}$ coronal sections were obtained from each breadloaf which was subsequently hematoxylin-eosin (H&E) stained. All H&E slides were captured with a BIOREVO BZ-9000 microscope (Keyence Corp., Osaka, Japan) and digitized at magnifications of x40, x200 and x400. To evaluate the change of the intrinsic muscles of the tongue, five consecutive H&E slides around the injection points per rabbit were analyzed in this study. To minimize that effect of the angle of the embedded tissue, we chose inferior longitudinal muscles (IL muscles) for the assessment, which runs from anterior to posterior side of the tongue (Fig. 2c). In x400 microscopic fields, the area and lesser diameter of each IL muscle fiber was measured with BZ-H1C and BZ-H1M software (Keyence Corp., Osaka, Japan), as described previously [13,14]. This software automatically measures the areas of the muscle fibers on a H&E slide (Fig. 2d). The muscle fibers, that were not sectioned vertically, were manually excluded.

To confirm the presence of Pax7, immunohistochemistry was performed with an automated staining platform (Ventana Discovery Ultra; Roche-Ventana Medical Systems,

Tucson, AZ, USA) using CC2 antigen retrieval buffer (Roche-Ventana) for 16 minutes at 100°C, followed by incubation with a rabbit anti-human Pax7 antibody (1:400 dilution; LS-B3490, LifeSpan BioSciences, Inc., Seattle, WA, USA) for 32 minutes at 36°C, followed by the OmniMap HRP multimer secondary detection system (Roche-Ventana).

Statistical Analysis

Data was analyzed using GraphPad Prism (Version 6.0c, GraphPad Software, La Jolla, CA, USA). Results are presented as mean \pm standard deviation (SD). The amount of food intake was scored using a 10-point scale with 10 being defined as all food eaten and 0 no food intake at all. The amounts of food intake, body weights and IL muscle fibers between the three groups were compared using a Kruskal-Wallis test with a Dunn's multiple comparison test as post hoc analyses. IL muscle fibers between the denervated and the non-denervated side was analyzed with a Mann-Whitney U-test. A p-value of <0.05 was considered statically significant.

RESULTS

Safety of the hyoglossus-denervated rabbit model

Following the denervation, none of the rabbits displayed adverse effects such as documented aspiration, surgical wound dehiscence and infection during follow-up. Under general anesthesia the tongue condition was carefully observed at 4 weeks after nerve transection. All rabbits had persistent fasciculation and strong atrophy in denervated side of the tongue, suggesting the success of the hyoglossus-denervated rabbit model.

The amount of food intake, or weight of the animals did not change over time

following denervation in none of the three groups at the 4 weeks after nerve transection. Following the injection therapy also none of the rabbits displayed adverse effects, nor did the body weight of the animals significantly change upon treatment at 8 weeks (Fig. 3). These results indicate the safety of the hyoglossus-denervated rabbit model.

Nerve transection causes atrophy of the intrinsic muscles in rabbits

We compared denervated and non-denervated sides of rabbit tongue in the control group (n=4) to confirm the effect of hypoglossal nerve transection. A representative tongue is shown in Fig. 4a, demonstrating strong atrophy on the denervated side, with pallor staining due to the muscle fiber atrophy and the presence of looser connective tissue. From the animals in the control group, a total of 20 H&E slides (5 per animal) were assessed with 1357 denervated IL muscle fibers and 1064 non-denervated IL muscle fibers analyzed. The denervated side of tongue had significantly smaller muscle fiber areas compared to the non-denervated side ($405\pm 220\mu\text{m}^2$ vs. $602\pm 28\mu\text{m}^2$, $p<0.05$). Similarly, significant smaller muscle fiber diameters were found in the denervated side compared to the non-denervated side ($20\pm 6\mu\text{m}$ vs. $25\pm 7\mu\text{m}$, $p<0.05$).

Hypertrophy of the intrinsic tongue muscle fiber with ADSCs in a tongue atrophy model

To assess the effect of fat injection therapy with ADSCs, we compared the areas and lesser diameters of IL muscles of the denervated side between the 3 groups (n=12) as shown in Fig. 4b. A total of 60 H&E slides from 12 rabbits (5 per animal) was assessed with 3780 denervated IL muscle fibers analyzed. Fig.5a shows representative IL muscle fibers from the ADSCs+fat, fat and control groups. Statistical analysis showed that the

ADSCs+fat group demonstrated a larger area of muscle fibers compared to the control and fat groups ($582\pm 312\mu\text{m}^2$ vs. $405\pm 220\mu\text{m}^2$ and $413\pm 226\mu\text{m}^2$, $p<0.05$) Similarly, a significant thicker lesser diameter of muscle fibers was found in the ADSCs+fat group compared to control and fat groups. ($24\pm 8\mu\text{m}$ vs. $20\pm 6\mu\text{m}$ and $20\pm 7\mu\text{m}$, $p<0.05$).

Immunohistochemistry of Pax7 demonstrated that more Pax7 positive cells were confirmed around the fat tissues in the ADSCs+fat group compared to the control group and the fat group (Fig. 5), suggesting that ADSCS differentiated into satellite cells and promoted the regeneration of muscle fibers around the injection area of the tongue.

DISCUSSION

Adipose-derived stem cells (ADSCs), similar to bone marrow mesenchymal stem cells, function as the precursors to fat cells but also have multipotency to differentiate into bone and cartilage mesenchymal cells [15-17]. For this, three elements, including cells, scaffold and growth factors, are essential for regeneration of tissue and organs and to achieve the prolonged effect of regenerative therapy [18]. In this study, ADSCs were injected into the atrophic tongue together with autologous fat tissue (scaffold and growth factors) to help tissue regeneration a in denervated area of the tongue. Animals that had received ADSCs demonstrated significant hypertrophied muscle fibers compared to control animals and animals that only received fat cells ($p<0.05$), indicating that ADSCs are essential to prevent the muscle atrophy after denervation. Moreover, the immunohistochemistry of Pax7 showed that the injected ADSCs might differentiate into satellite cells and promote the muscle regeneration around the injection area. Our result is consistent with the autologous muscle-derived stem cell (MDSC) injection therapy in a denervated tongue model, in which injected MDSCs survived and fused with tongue

myofibers, with a resultant increase in myofiber diameter and an increase in tongue strength [19]. The mechanism of tissue regeneration using the stem cell therapy appears to be as follows: (1) branching to vascular endothelial cells and stimulate vascularization; (2) emitting several growth factors including hepatocyte growth factor and vascular endothelial growth factor; (3) differentiating into muscle fiber and other tissues. The currently results are in line with a previous study in which we demonstrated that fat injection therapy with a high concentration of ADSCs in a paralyzed vocal cord animal model resulted in thyroarytenoid muscle fibers hypertrophy [8]. Our ADSCs injection treatment was evaluated in a preclinical model and been already applied into clinical trial with long-term efficacy and safety in patients with male stress urinary incontinence [20], making its application in patients with swallowing disorder a possibility in the near future. Because our surgical approach is similar to the fat injection therapy as performed in patients with unilateral vocal fold paralysis [9], the results from our study may thus be easily applied into a tongue or pharynx to increase the swallowing pressure at the stage of oral and pharynx phase.

The hypoglossal nerve is critical for movement of tongue in humans and its transection causes difficulty swallowing, and reduces swallowing pressure at the oropharynx [21,22], and arises from the ventrolateral side of the medulla oblongata with two main and divided into the lateral and medial main branches at the lateral aspect of the hypoglossal muscle [23]. All intrinsic and extrinsic muscles of the tongue are supplied by the hypoglossal nerve, with the exception of the palatoglossus. We selected rabbits as a tongue atrophy model to evaluate the safety and feasibility of fat injection therapy because the anatomy and the branching of the hypoglossal nerve in the rabbit is highly similar to

that of the human [24,25] and thus our model closely resembles the clinically encountered situation. Saito et al. assessed the anatomy of the intrinsic tongue muscles in rabbits and reported the three-dimensional ramification and intertwining of the transverse and vertical muscles [26]. In our study, the hypoglossal nerve was easily identified under submandibular gland without any surgical complications in all 12 rabbits and no subsequent adverse events were found in follow-up. Also, transection of the hypoglossal nerve demonstrated that intrinsic tongue muscle fibers in denervated side were significantly smaller than those in non-denervated side by performing histopathological analysis with H&E staining ($p < 0.05$, $405\mu\text{m}^2$ vs. $602\mu\text{m}^2$). These results show that the transection of hypoglossal nerve is feasible for hypoglossal denervated model in rabbits and is appropriate to evaluate the effect of the fat injection therapy as a preclinical model.

The timing of the injection therapy and histological evaluation was based on that from previous MDSCs injection therapies, in which the MDSCs were injected into the denervated thyroarytenoid muscle in a vocal fold paralysis model and the MDSC therapy attenuated muscle atrophy after laryngeal denervation [27,28]. Moreover, previous study demonstrated that the ADSCs and fat injection therapy increased blood flow to the mucous membrane of vocal folds in a vocal fold paralysis model at 4 weeks after the injection [8]. Several rabbit studies demonstrated that the timing of 8 weeks after nerve transection was feasible for the evaluation of atrophic muscles in a facial nerve paralysis model [29,30]. Taken together, we injected the ADSCs into the denervated side of the tongue at 4 weeks and evaluated the tongue at 8 weeks after the nerve transection.

There are some limitations to the clinical application of this technique. Firstly, we could not identify the actual injected fat with ADSCs in the denervated tongue. After

hypoglossal nerve transection, the muscle fibers in the denervated side of the tongue are thought to be atrophied and replaced into fat tissues during follow-up periods [31]. Although a larger area of fat tissue was found in the ADSCs+fat group after the injection therapy, to discriminate the injected fat with ADSCs from the replaced fat after denervation, cell labeling to ADSCs, such as PKH-26, might be needed in a future study. Secondly, we evaluated the safety and efficiency of fat injection with ADSCs in rabbit hypopharyngeal paralysis model, however, the changes during follow-up were short (8 weeks) and insufficient to evaluate the regeneration of the tissue. To evaluate the role of the ADSCs in denervated tongue, further preclinical study is required with long-term observational period.

CONCLUSION

The rabbit tongue atrophy model was found suitable for the assessment of muscle change after nerve transection. Fat injection therapy with ADSCs demonstrated great potential to prevent the muscle atrophy after denervation and to promote the muscle regeneration around the injection area.

Disclosure statement

The authors have no financial conflicts of interest to declare

Acknowledgements

This work was supported in part by a Japan Society for the Promotion of Science Grant-in-Aid for Young Scientists (B) JP17K16906. We thank Kumiko Yano for animal care; Makiko Kato for cell culture; and the Division for Medical Research Engineering,

Nagoya University Graduate School of Medicine, for technical support.

References

- [1] Clavé P, Shaker R. Dysphagia: current reality and scope of the problem. *Nat Rev Gastroenterol Hepatol* 2015;12:259–70.
- [2] Barczy SR, Sullivan PA, Robbins J. How should dysphagia care of older adults differ? Establishing optimal practice patterns. *Semin Speech Lang* 2000;21:347–61.
- [3] Matsuo K, Palmer JB. Anatomy and physiology of feeding and swallowing: normal and abnormal. *Phys Med Rehabil Clin N Am* 2008;19:691–707.
- [4] Fujimoto Y, Hasegawa Y, Yamada H, Ando A, Nakashima T. Swallowing function following extensive resection of oral or oropharyngeal cancer with laryngeal suspension and cricopharyngeal myotomy. *Laryngoscope* 2007;117:1343–8.
- [5] Shama L, Connor NP, Ciucci MR, McCulloch TM. Surgical treatment of dysphagia. *Phys Med Rehabil Clin N Am* 2008;19:817–35.
- [6] Mazzola RF, Cantarella G, Torretta S, Sbarbati A, Lazzari L, Pignataro L. Autologous fat injection to face and neck: from soft tissue augmentation to regenerative medicine. *Acta Otorhinolaryngol Ital* 2011;31:59–69.
- [7] Mikaelian DO, Lowry LD, Sataloff RT. Lipoinjection for unilateral vocal cord paralysis. *Laryngoscope* 1991;101:465–8.
- [8] Nishio N, Fujimoto Y, Suga K, Iwata Y, Toriyama K, Takanari K, et al. Autologous fat injection therapy including a high concentration of adipose-derived regenerative cells in a vocal fold paralysis model: animal pilot study. *J Laryngol Otol* 2016;130:914–22.
- [9] Nishio N, Fujimoto Y, Hiramatsu M, Maruo T, Suga K, Tsuzuki H, et al.

Computed tomographic assessment of autologous fat injection augmentation for vocal fold paralysis. *Laryngoscope Investig Otolaryngol* 2017;2:459–65.

[10] Navach V, Calabrese LS, Zurlo V, Alterio D, Funicelli L, Giugliano G. Functional base of tongue fat injection in a patient with severe postradiation Dysphagia. *Dysphagia* 2011;26:196–9.

[11] Kraaijenga SAC, Lapid O, van der Molen L, Hilgers FJM, Smeele LE, van den Brekel MWM. Feasibility and potential value of lipofilling in post-treatment oropharyngeal dysfunction. *Laryngoscope* 2016;126:2672–8.

[12] Silwal Gautam S, Imamura T, Ishizuka O, Lei Z, Yamagishi T, Yokoyama H, et al. Implantation of autologous adipose-derived cells reconstructs functional urethral sphincters in rabbit cryoinjured urethra. *Tissue Eng Part A* 2014;20:1971–9.

[13] Ohnishi M, Tsuge M, Kohno T, Zhang Y, Abe H, Hyogo H, et al. IL28B polymorphism is associated with fatty change in the liver of chronic hepatitis C patients. *J Gastroenterol* 2012;47:834–44.

[14] Ohno S, Hirano S, Kanemaru S, Mizuta M, Ishikawa S, Tateya I, et al. Role of circulating MSCs in vocal fold wound healing. *Laryngoscope* 2012;122:2503–10.

[15] Zuk PA, Zhu M, Mizuno H, Huang J, Futrell JW, Katz AJ, et al. Multilineage cells from human adipose tissue: implications for cell-based therapies. *Tissue Eng* 2001;7:211–28.

[16] Safford KM, Hicok KC, Safford SD, Halvorsen Y-DC, Wilkison WO, Gimble JM, et al. Neurogenic differentiation of murine and human adipose-derived stromal cells. *Biochem Biophys Res Commun* 2002;294:371–9.

[17] Fraser JK, Wulur I, Alfonso Z, Hedrick MH. Fat tissue: an underappreciated

source of stem cells for biotechnology. *Trends Biotechnol* 2006;24:150–4.

[18] Lee BJ, Wang SG, Lee JC, Jung JS, Bae YC, Jeong HJ, et al. The prevention of vocal fold scarring using autologous adipose tissue-derived stromal cells. *Cells Tissues Organs* 2006;184:198–204.

[19] Plowman EK, Bijangi-Vishehsaraei K, Halum S, Cates D, Hanenberg H, Domer AS, et al. Autologous myoblasts attenuate atrophy and improve tongue force in a denervated tongue model: a pilot study. *Laryngoscope* 2014;124:20–6.

[20] Gotoh M, Yamamoto T, Shimizu S, Matsukawa Y, Kato M, Majima T, et al. Treatment of male stress urinary incontinence using autologous adipose-derived regenerative cells: Long-term efficacy and safety. *Int J Urol* 2019;26:400–5.

[21] Elfring T, Boliek CA, Winget M, Paulsen C, Seikaly H, Rieger JM. The relationship between lingual and hypoglossal nerve function and quality of life in head and neck cancer. *J Oral Rehabil* 2014;41:133–40.

[22] Tsujimura T, Suzuki T, Yoshihara M, Sakai S, Koshi N, Ashiga H, et al. Involvement of hypoglossal and recurrent laryngeal nerves on swallowing pressure. *J Appl Physiol* 2018;124:1148–54.

[23] Ateş S, Karakurum E, Dursun N. Origin, course and distribution of the hypoglossal nerve in the New Zealand rabbit (*Oryctolagus cuniculus* L). *Anat Histol Embryol* 2011;40:360–4.

[24] Delaey P, Duisit J, Behets C, Duprez T, Gianello P, Lengelé B. Specific branches of hypoglossal nerve to genioglossus muscle as a potential target of selective neurostimulation in obstructive sleep apnea: anatomical and morphometric study. *Surg Radiol Anat* 2017;39:507–15.

- [25] Benderro GF, Gamble J, Schiefer MA, Baskin JZ, Hernandez Y, Strohl KP. Hypoglossal nerve stimulation in a pre-clinical anesthetized rabbit model relevant to OSA. *Respir Physiol Neurobiol* 2018;250:31–8.
- [26] Saito H, Itoh I. Three-dimensional architecture of the intrinsic tongue muscles, particularly the longitudinal muscle, by the chemical-maceration method. *Anat Sci Int* 2003;78:168–76.
- [27] Halum SL, Naidu M, Delo DM, Atala A, Hingtgen CM. Injection of autologous muscle stem cells (myoblasts) for the treatment of vocal fold paralysis: a pilot study. *Laryngoscope* 2007;117:917-22.
- [28] Halum SL, Hiatt KK, Naidu M, Sufyan AS, Clapp DW. Optimization of autologous muscle stem cell survival in the denervated hemilarynx. *Laryngoscope* 2008;118:1308-12.
- [29] Tulaci KG, Tuzuner A, Karadas Emir H, Tatar İ, Sargon MF, Tulaci T, et al. The effect of tacrolimus on facial nerve injury: Histopathological findings in a rabbit model. *Am J Otolaryngol* 2016;37:393-7.
- [30] Sereflican M, Yurttas V, Ozyalvacli G, Terzi EH, Turkoglu SA, Yildiz S, et al. The histopathological and electrophysiological effects of thymoquinone and methylprednisolone in a rabbit traumatic facial nerve paralysis model. *Am J Otolaryngol* 2016;37:407-15.
- [31] Ho TL, Lee KW, Lee HJ. Subacute mandibular and hypoglossal nerve denervation causing oedema of the masticator space and tongue. *Neuroradiology* 2003;45:262-6.

Figure Legends

Figure 1: Study workflow (a). Surgical procedure including transection of hypoglossal nerve (b) and fat injection therapy for tongue (c,d). White arrow: Hypoglossal nerve.

Figure 2: Histological assessment of the intrinsic muscles of the tongue

Rabbit tongues were breadloafed in 5mm thick tissue sections in the coronal plane from the tongue tip to tongue base (a,b). Within the intrinsic muscles of the tongue, inferior longitudinal muscles were chosen for the histological assessment (c). The areas and diameter of the inferior longitudinal muscle fibers were measured on a hematoxylin-eosin slide (d). Scale bars = 100 μ m.

Figure 3: Change of body weight in three groups during follow-up periods (n=12)

Figure 4: Strong muscle atrophy of inferior longitudinal muscles is seen on the denervated side in the control group (a). Compared to the fat group and the control group, significant hypertrophy of the inferior longitudinal muscle fibers is found in the ADSCs+fat group (b). Scale bars = 100 μ m. IL: inferior longitudinal muscle.

Figure 5: Immunohistochemistry of Pax7 demonstrated that more Pax7 positive cells were confirmed around the fat tissues in the ADSCs+fat group compared to the control group and the fat group. Scale bars = 100 μ m.

a

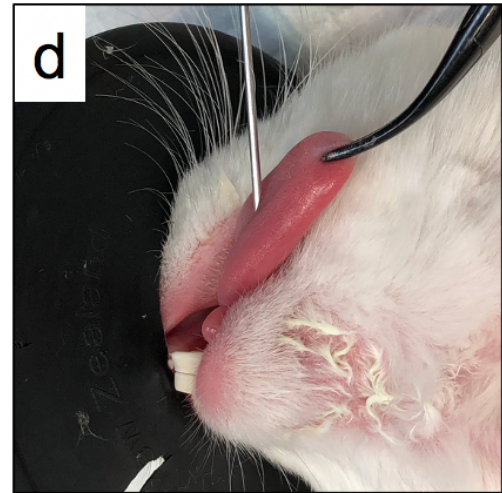
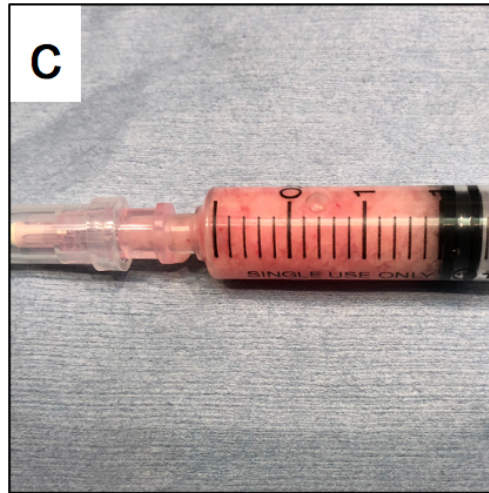
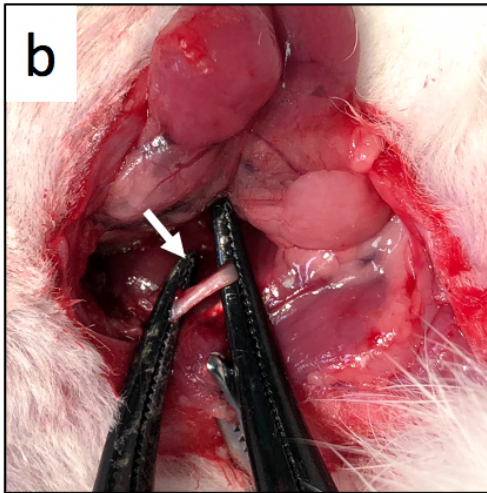
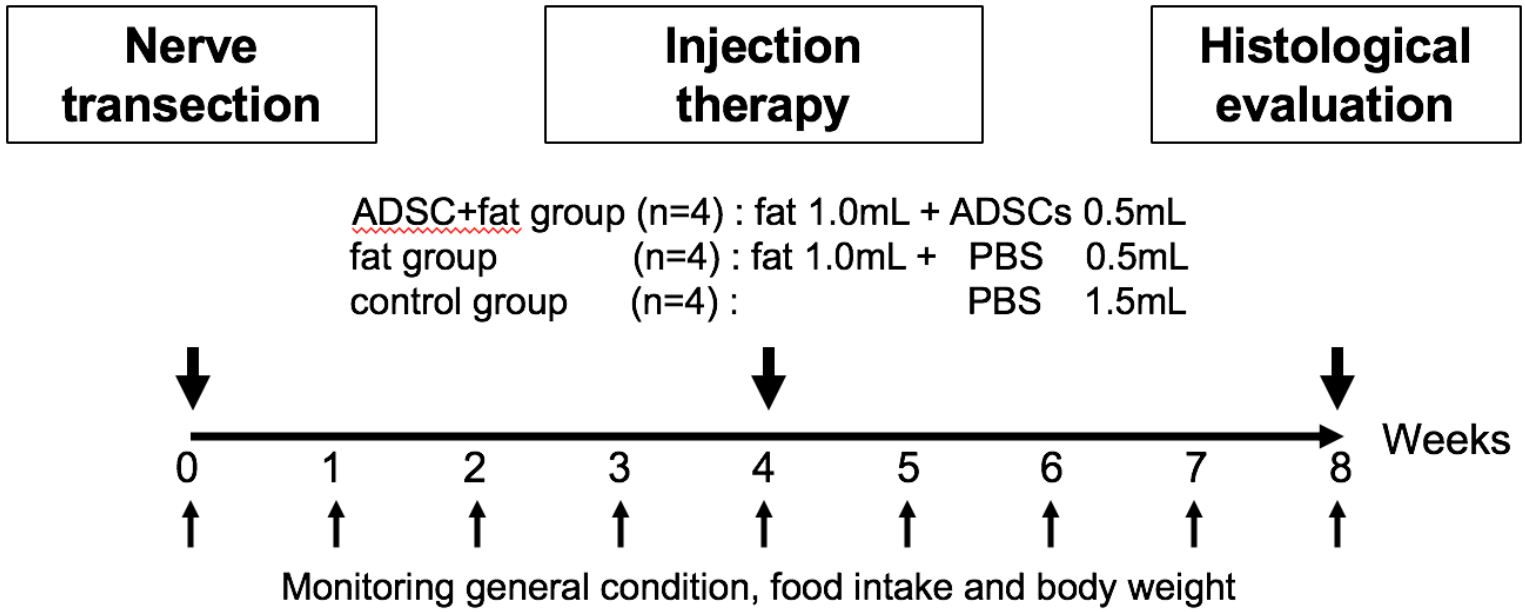


Figure 2

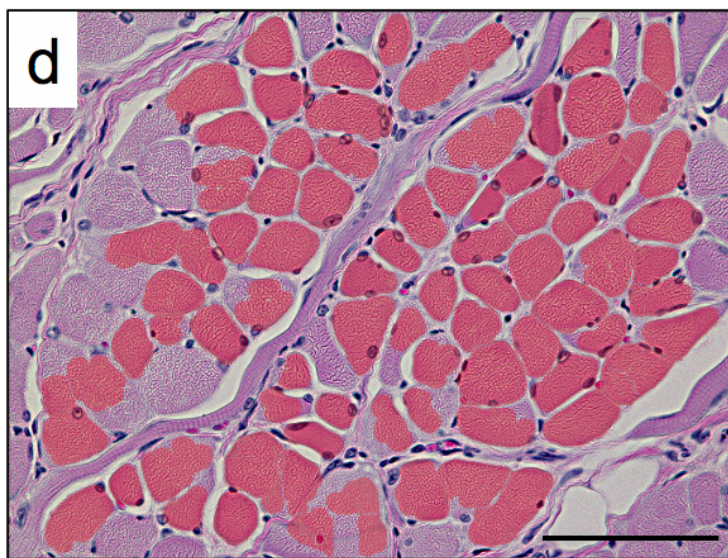
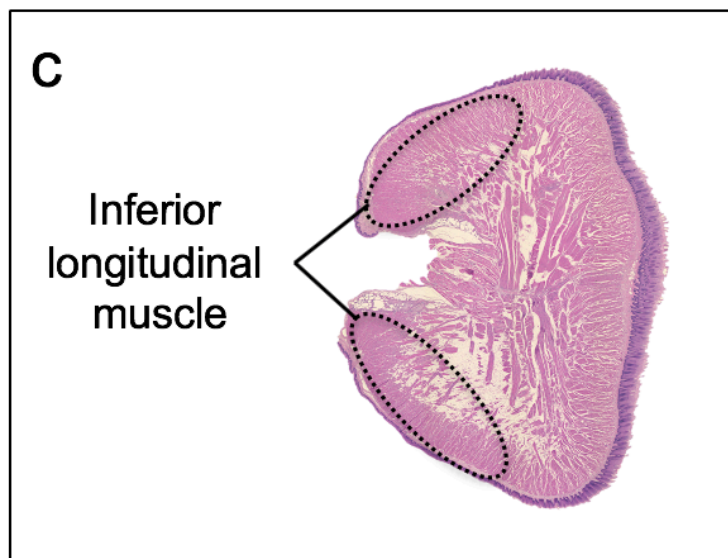
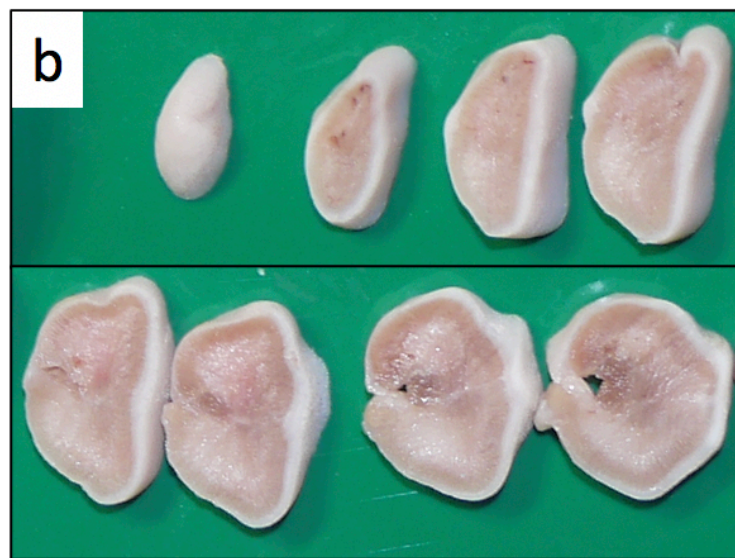
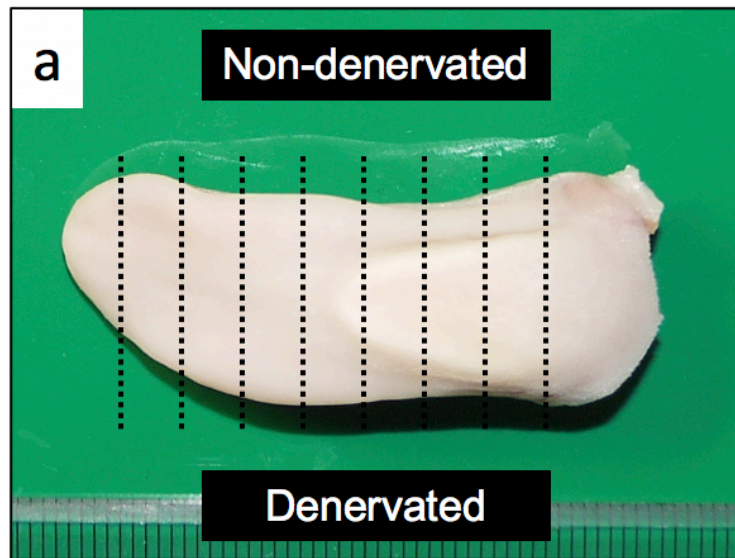


Figure 3

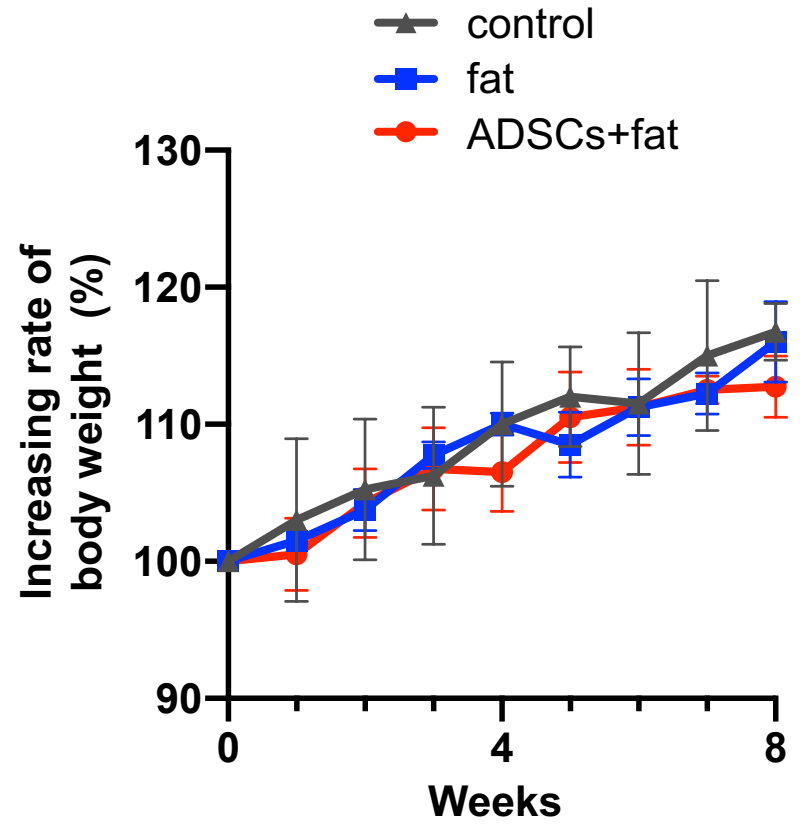
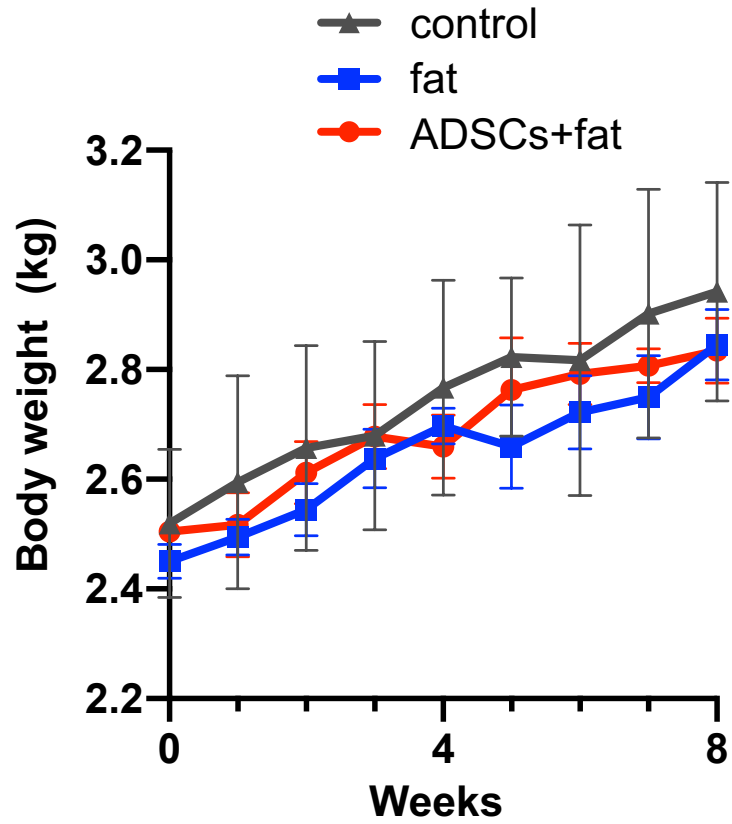


Figure 4

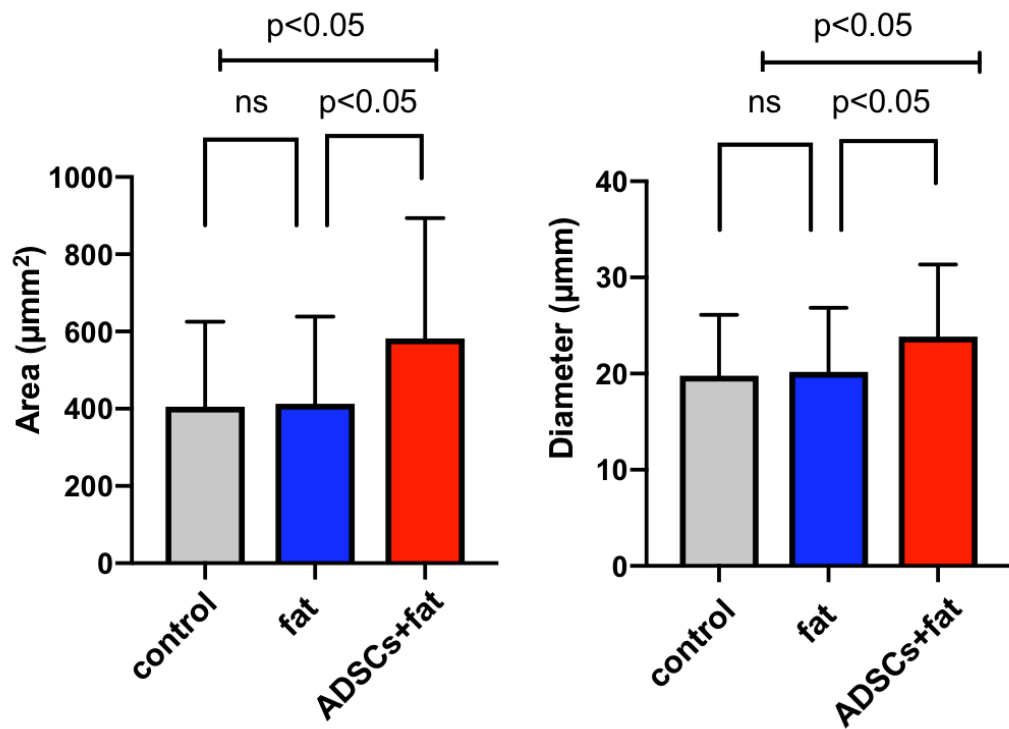
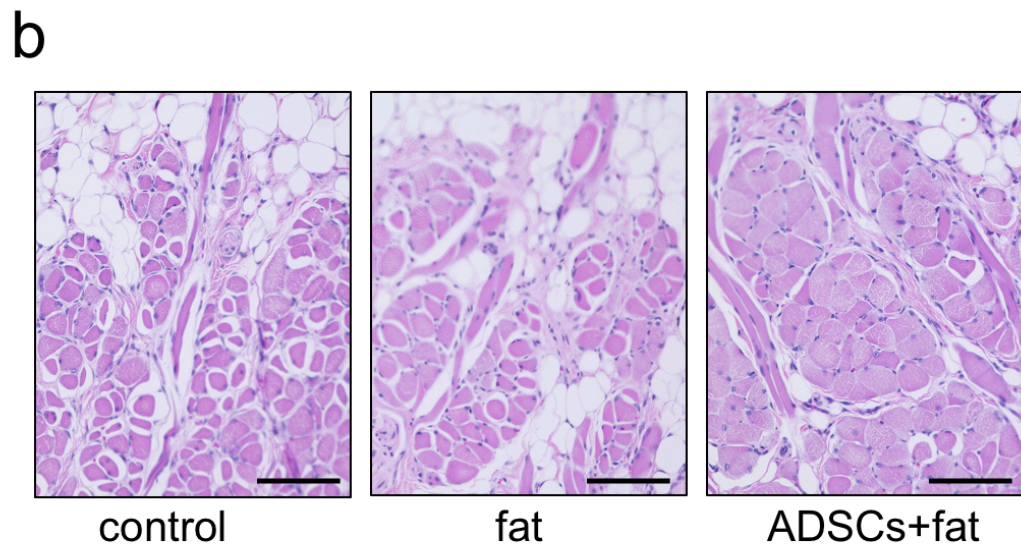
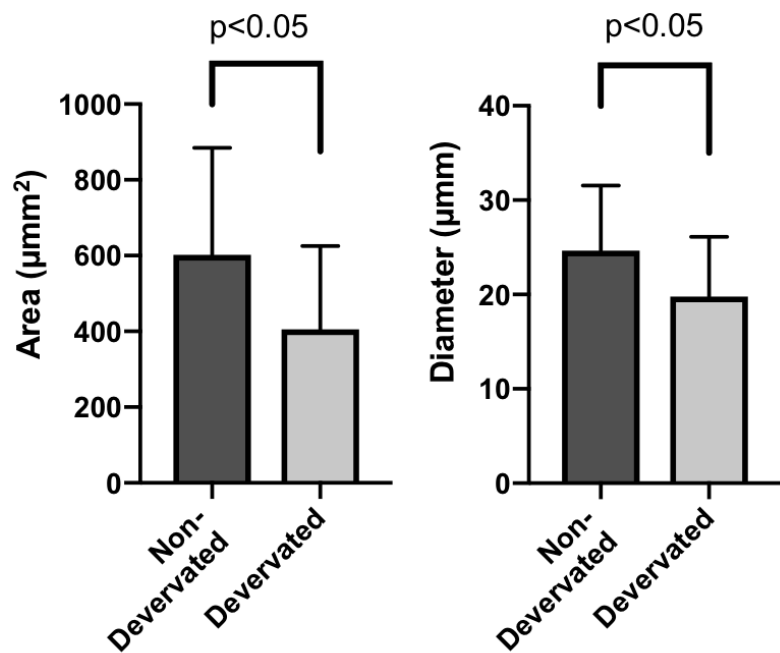
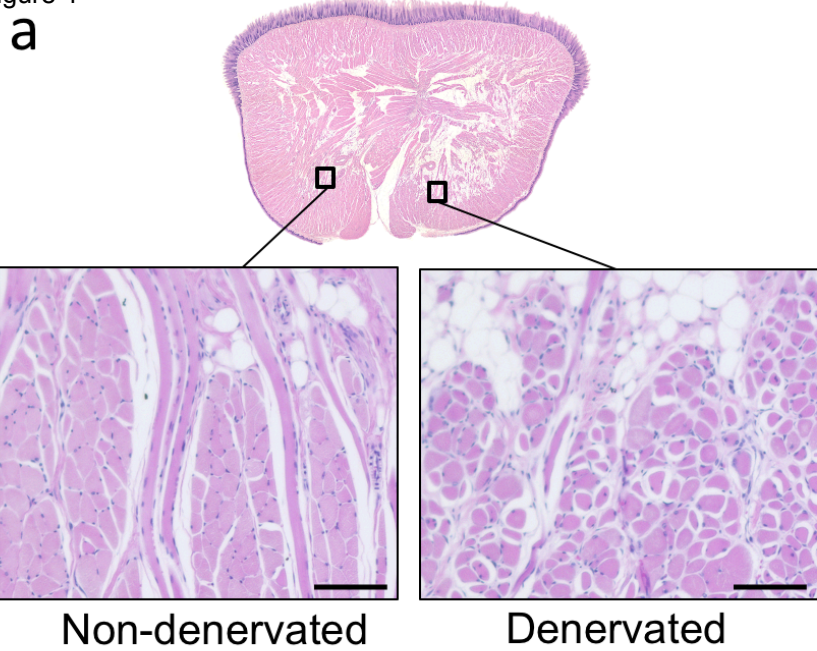
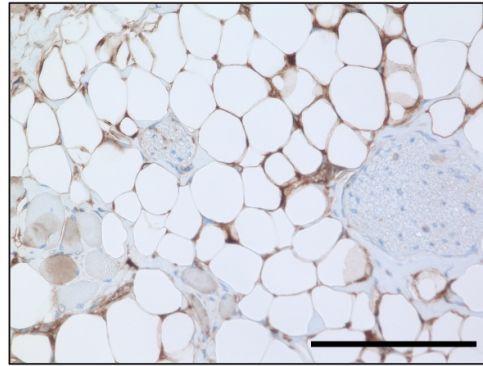
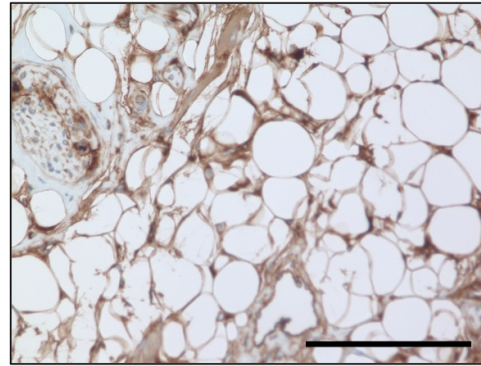


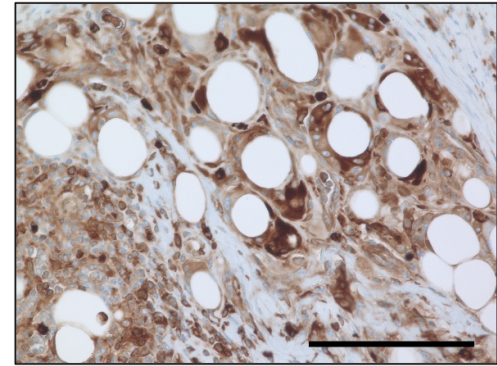
Figure 5



control



fat



ADSCs+fat